

**UCLA**

**UCLA Electronic Theses and Dissertations**

**Title**

CO2 Conversion by Reverse Water Gas Shift Reaction

**Permalink**

<https://escholarship.org/uc/item/7bn2658j>

**Author**

Alamer, Abdulaziz

**Publication Date**

2018

Peer reviewed|Thesis/dissertation

UNIVERSITY OF CALIFORNIA

Los Angeles

CO<sub>2</sub> Conversion by  
Reverse Water Gas Shift Reaction

A thesis submitted in partial satisfaction  
of the requirements for the degree Master of Science  
in Chemical Engineering

by

Abdulaziz Mohammed A Alamer

2018

© Copyright by

Abdulaziz Mohammed A Alamer

2018

## ABSTRACT OF THE THESIS

CO<sub>2</sub> Conversion by  
Reverse Water Gas Shift Reaction

by

Abdulaziz Mohammed A Alamer

Master of Science in Chemical Engineering  
University of California, Los Angeles, 2018  
Professor Vasilios Manousiouthakis, Chair

In recent decades, the world has been concerned about the environmental impact of CO<sub>2</sub> emissions into the atmosphere. Thus, researchers have been focusing on enhancing current technologies, such as the Reverse Water Gas Shift (RWGS) reaction, to convert CO<sub>2</sub> to synthetic fuels. The goal of this research was to develop a catalyst that has a high CO<sub>2</sub> conversion and CO selectivity. To achieve this goal, different experiments were conducted at the same conditions to study the effect of different supports, metal loadings and different metals. All the experimental results were compared to equilibrium data obtained from Aspen Plus. Each tested catalyst was analyzed by BET and XRD to understand its physical and chemical structure as well as its behavior. Best catalyst was identified to be 5 wt% Cu supported on MgO, which achieved 20% CO<sub>2</sub> conversion, 84% of Equilibrium CO<sub>2</sub> conversion, and 75% CO selectivity.

The thesis of Abdulaziz Mohammed A Alamer is approved.

Yunfeng Lu

Dante A Simonetti

Vasilios Manousiouthakis, Committee Chair

University of California, Los Angeles

2018

## TABLE OF CONTENTS

<b>CHAPTER 1. INTRODUCTION.....</b>	<b>1</b>
<b>1.1 Motivation.....</b>	<b>1</b>
<b>1.2 Background .....</b>	<b>4</b>
<b>1.3 Objective .....</b>	<b>8</b>
<b>CHAPTER 2. METHODOLOGY .....</b>	<b>9</b>
<b>2.1 Experimental Apparatus.....</b>	<b>9</b>
2.1.1 High Throughput.....	9
2.1.2 Micro-Reactor .....	10
2.1.3 Feed Gas Control System.....	11
2.1.4 Gas Chromatography System.....	11
<b>2.2 Experimental Procedure .....</b>	<b>12</b>
2.2.1 Catalyst Preparation .....	13
2.2.2 Type of Experiments .....	14
<b>CHAPTER 3. EXPERIMENTAL RESULTS AND DISCUSSION.....</b>	<b>16</b>
<b>3.1 The Effect of Support .....</b>	<b>19</b>
<b>3.2 The Effect of Metal Loading .....</b>	<b>21</b>
<b>3.3 The Effect of Different Types of Metals.....</b>	<b>23</b>
<b>CHAPTER 4. CONCLUSIONS AND RECOMMENDATIONS.....</b>	<b>26</b>
<b>4.1 Conclusions.....</b>	<b>26</b>
<b>4.2 Recommendations for Future Work.....</b>	<b>27</b>
<b>REFERENCES .....</b>	<b>28</b>

## LIST OF FIGURES

Figure 1: Monthly Average Atmospheric CO <sub>2</sub> Concentration (PPM) Versus Time in Mauna Loa Observatory, Hawaii <sup>[1]</sup> . (© Scripps CO <sub>2</sub> Program 2017) .....	1
Figure 2: Percentage of Different Human Activities that Contribute to Climate Change <sup>[4]</sup> . (© Intergovernmental Panel on Climate Change 2014) .....	2
Figure 3: The process of Carbon Capture and Storage (CCS) .....	3
Figure 4: Effect of temperature on the thermodynamic equilibrium of the RWGS reaction <sup>[11]</sup> .....	5
Figure 5: High Throughput System .....	9
Figure 6: High Throughput Micro-Reactor System .....	10
Figure 7: Wells Containing Individual Catalyst Pellets or Powders .....	10
Figure 8: Mass Flow Controller Set-up .....	11
Figure 9: Agilent Micro Gas Chromatography (GC) .....	12
Figure 10: Schematic of the Gibbs Reactor .....	16
Figure 11: CO <sub>2</sub> Equilibrium Conversion .....	17
Figure 12: CO <sub>2</sub> Conversion for Different Support .....	19
Figure 13: CO Selectivity for Different Support .....	20
Figure 14: XRD Spectrum for 10 wt% Cu/SiO <sub>2</sub> .....	21
Figure 15: XRD Spectrum for 10 wt% Cu/MgO .....	21
Figure 16: CO <sub>2</sub> Conversion for Different Metal Loading .....	22
Figure 17: CO Selectivity for Different Metal Loading .....	23
Figure 18: CO <sub>2</sub> Conversion for Different Metals .....	24
Figure 19: CO Selectivity for Different Metals .....	25
Figure 20: XRD Spectrum for 5 wt% Cu/MgO .....	25

## LIST OF TABLES

Table 1: Catalyst Prepared for this Project	14
Table 2: The Actual Metal Percentage Loaded for each Prepared Catalyst	18



## ACKNOWLEDGEMENTS

I would like to first thank professor Vasilios Manousiouthakis, my advisor and committee chairman, for all of the support and guidance he has provided. He helped me manage the project and overcome obstacles. I would also like to thank professor Dante Simonetti and professor Yunfeng Lu for using their lab and facilities to conduct the research. This project would not have been possible without the assistance of friends and colleagues. Thus, I would like to thank my friends and colleagues, especially my friend, Faisal Alshafei, for their support. Last but not least, my heartfelt appreciation goes to my family for their support and to my wife for her patience and encouragement.

## CHAPTER 1. INTRODUCTION

### 1.1 Motivation

The concentration of carbon dioxide (CO<sub>2</sub>) in the atmosphere has been increasing since the industrial revolution. As of now, it has surpassed 400 parts per million (ppm), as shown in Figure 1<sup>[1]</sup>. This pattern is expected to continue, and to reach 1000 ppm by 2100<sup>[2]</sup>. In 2015, the emissions of CO<sub>2</sub> into the atmosphere were 32294 megatonnes (Mt), and it is expected to increase to 45000 Mt by 2040<sup>[3]</sup>. This increase can lead to changes to the earth's climate.

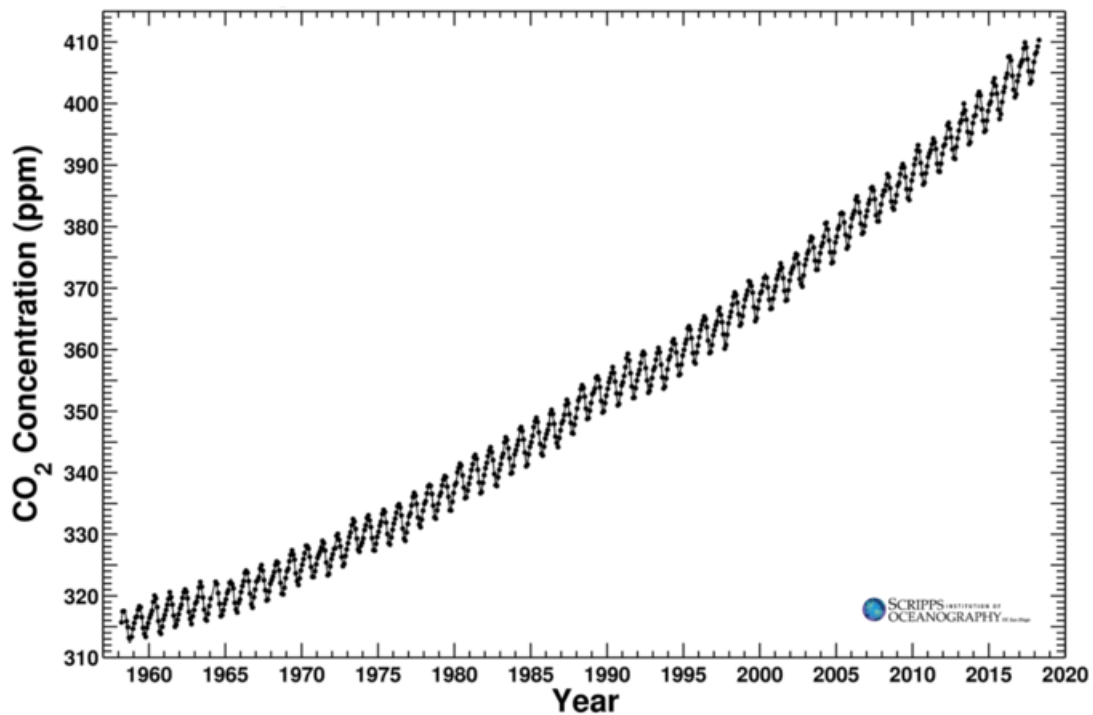


**Figure 1:** Monthly Average Atmospheric CO<sub>2</sub> Concentration (PPM) Versus Time in Mauna Loa Observatory, Hawaii<sup>[1]</sup>. (© Scripps CO<sub>2</sub> Program 2017)

According to the Intergovernmental Panel on Climate Change (IPCC), the percentage of different human activities that contribute to changing the composition of

the earth's atmosphere and potentially impacting its climate, are shown in Figure 2 <sup>[4]</sup>. Carbon dioxide emissions through burning fossil fuels and industrial processes are the highest contributors, followed by methane and nitrous oxide emissions from agriculture. A large amount of the CO<sub>2</sub> emissions is absorbed into the oceans causing its pH levels to decrease, thus threatening the ocean's native organisms <sup>[5]</sup>.

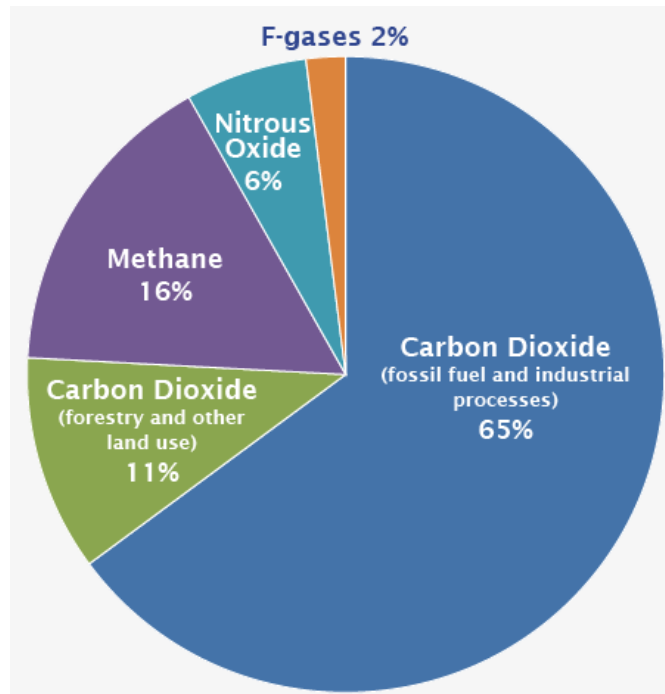


**Figure 2:** Percentage of Different Human Activities that Contribute to Climate Change

<sup>[4]</sup>. (© Intergovernmental Panel on Climate Change 2014)

Due to the rapidly increasing CO<sub>2</sub> atmospheric concentrations, extensive research is being conducted to reduce CO<sub>2</sub> emissions into the atmosphere. Part of the research focuses on capturing and storing CO<sub>2</sub>, whereas another part emphasizes the reuse of CO<sub>2</sub> as a carbon source to produce chemicals and fuels.

The most common method to capture CO<sub>2</sub> and store it is Carbon Capture and Storage (CCS) or known as sequestration. CCS captures and separates CO<sub>2</sub> from other

gases produced in electricity generation and industrial processes using one of three methods: pre-combustion capture, post-combustion capture or oxyfuel combustion. CO<sub>2</sub> is then transported for safe storage by pipelines, road tankers or ships. Finally, CO<sub>2</sub> is stored in depleted oil and gas fields or deep saline aquifer formations several kilometers below the earth's surface <sup>[6]</sup>. Figure 3 shows the process of capturing and storing CO<sub>2</sub> using CCS. It is projected that using CCS can store about 3 gigatonnes (Gt) a year of CO<sub>2</sub> by 2031 <sup>[7]</sup>. This method is effective in storing CO<sub>2</sub>; however, it is costly and CO<sub>2</sub> storage is not sustainable, as at some point there will be no more space to store CO<sub>2</sub>.

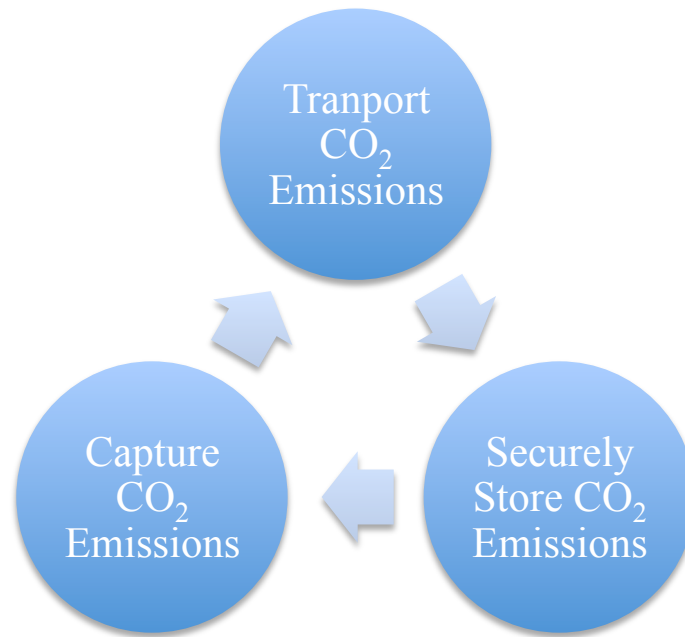


**Figure 3:** The process of Carbon Capture and Storage (CCS)

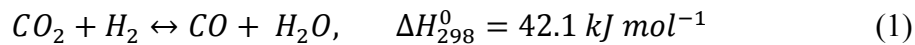
Recently, many researches are being conducted on reusing CO<sub>2</sub> emissions as a carbon source to produce high value chemicals and fuels. This process is called Carbon Capture and Utilization (CCU) and is less costly (or even profitable) than CCS. In order for CCU to be more effective than CCS, it has to be renewable resulting in neutral or

negative carbon emissions. The issue facing CCU is the stability of the CO<sub>2</sub> molecule, which requires high temperatures, hydrogen and catalysts to break the C=O bond [8].

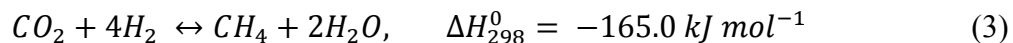
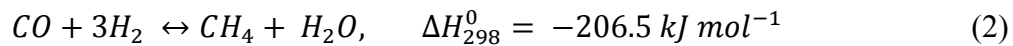
## 1.2 Background

There are multiple technologies that focus on converting CO<sub>2</sub> to synthetic fuels. Some of these technologies are the Reverse Water Gas Shift (RWGS) reaction, the dry reforming of methane, and the direct hydrogenation of CO<sub>2</sub> to chemicals. RWGS is an endothermic reaction and represents an important route to CO formation, which is considered a building block for a variety of chemicals [9]. The RWGS reaction also plays a key role in the selective methanation of CO<sub>2</sub> and in methanol synthesis from syngas [10]. Thus, RWGS is a key reaction and needs to be understood and researched.

The RWGS reaction is limited by equilibrium, and given its endothermic nature, shown in Equation 1, it requires at high operating temperature.



Side reactions of RWGS include the Methanation reaction, equation 2, and the Sabatier reaction, equation 3.



The effect of temperature on the thermodynamic equilibrium of the RWGS reaction is shown in Figure 4 [11]. The CO<sub>2</sub> conversion in the RWGS reaction is enhanced when excess H<sub>2</sub> is fed and temperature is increased. Almost 100% CO<sub>2</sub> conversion can be achieved when a membrane reactor is used to separate the products and shifts the

equilibrium toward the products <sup>[12]</sup>.

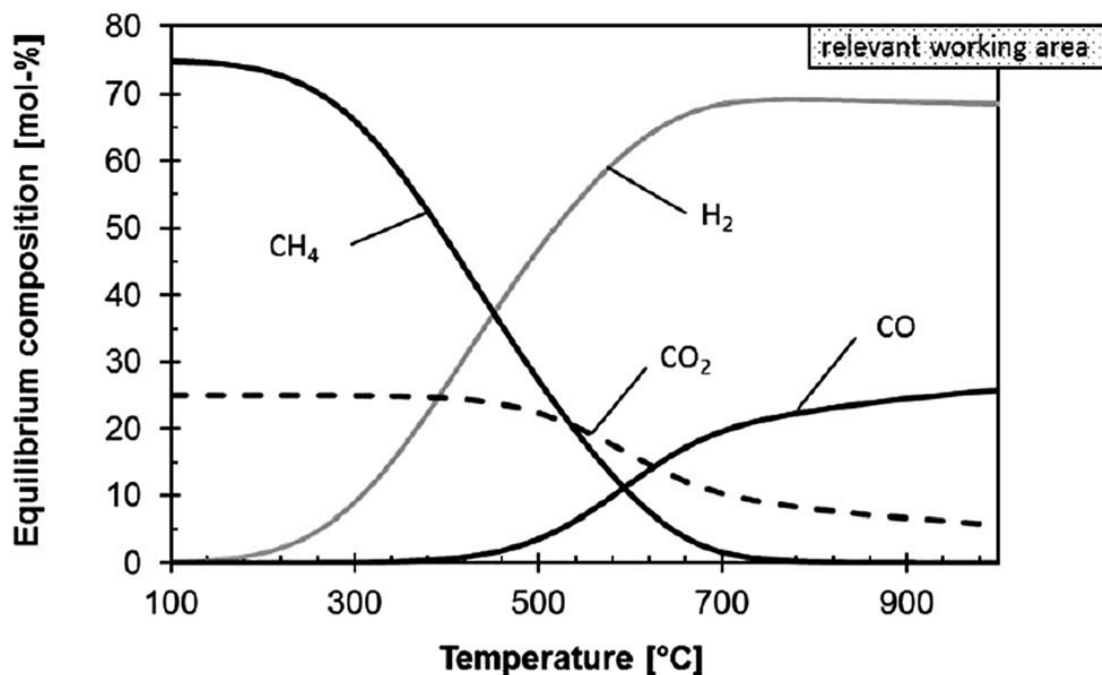


**Figure 4:** Effect of temperature on the thermodynamic equilibrium of the RWGS reaction <sup>[11]</sup>

Over the last two decades, nanoparticles have been extensively used in heterogeneous catalysis, since nano-catalysts have more surface area and active sites thus increasing catalyst activity <sup>[13]</sup>. Depending on the synthesis method used, nano-catalysts with different particle shapes and distributions are obtained. Research has proven that catalysts that are good for a forward reaction are likely to be good for the reverse reaction <sup>[14]</sup>. These catalysts include platinum, rhodium, nickel and copper.

Given their ability to dissociate H<sub>2</sub> atoms, supported noble metals such as platinum (Pt) have been known to be active catalysts for CO<sub>2</sub> hydrogenation and have been used to attain good CO<sub>2</sub> conversion in the RWGS reaction <sup>[15]</sup>. Pt supported on titanium oxide (TiO<sub>2</sub>) was tested for the RWGS reaction, at different temperatures and

H<sub>2</sub>:CO<sub>2</sub> ratios; near CO<sub>2</sub> equilibrium conversion was achieved for the tested temperature [15]. The effect of different supports on CO<sub>2</sub> conversion was studied and showed that Pt supported on TiO<sub>2</sub> results in an increased CO<sub>2</sub> conversion compared to gamma-alumina (γ-Al<sub>2</sub>O<sub>3</sub>) support [16]. Research has shown that Pt supported on Lanthanum (La) and Zirconium Oxide (ZrO<sub>2</sub>) resulted in higher CO<sub>2</sub> conversion compared to other supported metals, such as copper and iron [17]. Despite the multiple advantages the Pt catalyst offers, its high cost restricts its use as an effective industrial catalyst.

Nickel (Ni) has been extensively studied for the RWGS reaction due to its stability at high temperatures. Ni on cerium oxide (CeO<sub>2</sub>) catalysts were tested at high temperatures (400-750 °C) to study the effect of Ni loading on the RWGS reaction [18]. Different Ni loading (0-20 %) was tested and it was found that 2% wt resulted in 100% CO selectivity and the best CO<sub>2</sub> conversion; whereas, high Ni loading resulted in lowering CO selectivity [19]. The experiments showed that oxygen vacancies formed on ceria's crystal lattices and highly dispersed Ni particles increased CO<sub>2</sub> conversion [18]. Ni and Cu system support on γ-Al<sub>2</sub>O<sub>3</sub> was also tested for the RWGS reaction, and it was observed that increasing Ni loading did not affect CO<sub>2</sub> conversion but lowered CO selectivity [19]. Ni is well known to be a high selective catalyst toward CH<sub>4</sub> and it further hydrogenates CO to CH<sub>4</sub>; however, it remains a good candidate for the RWGS reaction, when it operates at high temperatures, since the methanation reaction is less favorable at these temperatures [21].

Rhodium (Rh) is often used as a homogenous catalyst for CO<sub>2</sub> hydrogenation, and supported Rh is used as a heterogeneous catalyst for CO<sub>2</sub> hydrogenation. Rh support on

TiO<sub>2</sub> was tested for the RWGS reaction at 200 °C, and it was observed that CO selectivity increased at low Rh loading, due to the isolated Rh on the surface of the support <sup>[22]</sup>. CO formation rates on Rh supported on TiO<sub>2</sub> increased two orders of magnitude, when compared to MgO, Nb<sub>2</sub>O<sub>5</sub> and ZrO<sub>2</sub> as supports <sup>[23]</sup>. Also, researchers found that adding Iron (Fe) to Rh/TiO<sub>2</sub> enhances CO selectivity, but lowers CO<sub>2</sub> conversion <sup>[24]</sup>. Different metal precursors used in the catalyst preparation also affect catalyst activity and selectivity. Rh supported on silica oxide (SiO<sub>2</sub>) synthesized from nitrate and acetate precursors resulted in catalysts that are more selective toward CO, whereas the ones from a chloride precursor resulted in a catalyst that is more selective toward CH<sub>4</sub> <sup>[25]</sup>.

Copper (Cu) is the most studied catalyst for the water gas shift (WGS) reaction. Cu based catalysts have the advantage of being cheap compared to other noble metals, and favor the formation of CO over other products such as methane <sup>[26]</sup>. Cu/CeO<sub>2</sub> was synthesized and tested for the RWGS reaction, showing 100% CO selectivity and good CO<sub>2</sub> conversion <sup>[27]</sup>. The effect of promoters in Cu/SiO<sub>2</sub> was also studied, and it was observed that the addition of promoters enhances the catalyst activity overall <sup>[28]</sup>. The addition of potassium (K) increased active site surface, whereas the addition of Iron (Fe) increased the catalyst stability at high temperature <sup>[29]</sup>. To increase the activity of the Cu, based catalyst ZnO, Fe<sub>2</sub>O<sub>3</sub> and Cr<sub>2</sub>O<sub>3</sub> have all been used to dope Cu <sup>[30]</sup>. Researchers observed a linear relationship between the catalyst activity and the surface area of metallic Cu <sup>[31]</sup>. Cu catalyst is known to sinter at high temperature due to its low melting point, and one way to overcome this issue is to prepare Cu/SiO<sub>2</sub> catalyst by atomic layer epitaxy (ALE), which helps in forming small Cu particles <sup>[32]</sup>.



### 1.3 Objective

Considering the undesirable effects of CO<sub>2</sub> emissions on the atmosphere, the objective of this research was to develop a stable and active catalyst that is selective to CO formation via the Reverse Water Gas Shift Reaction (RWGSR). In order to develop an active catalyst, a set of experiments was performed to study the effect of different parameters on the catalyst activity toward high CO<sub>2</sub> conversion and CO selectivity. These parameters are:

1. Effect of different supports for Cu based catalyst at moderate reaction conditions.
2. Effect of different metal loadings in enhancing CO<sub>2</sub> conversion and CO selectivity.
3. Effect of different metals on CO<sub>2</sub> conversion and CO selectivity.

## CHAPTER 2. METHODOLOGY

### 2.1 Experimental Apparatus

#### 2.1.1 High Throughput

The major apparatus used in this experiment is a high throughput reactor, shown in Figure 5. The main four components of the high throughput are: feed gas system that includes several MKS flow meters, pressure regulator and mixing tube, micro-reactor system that is mounted on top of a x-y-z motion system, heating system that includes heating cartridges and Eurotherm PID controllers, and analysis instruments that include microGC 490 systems.

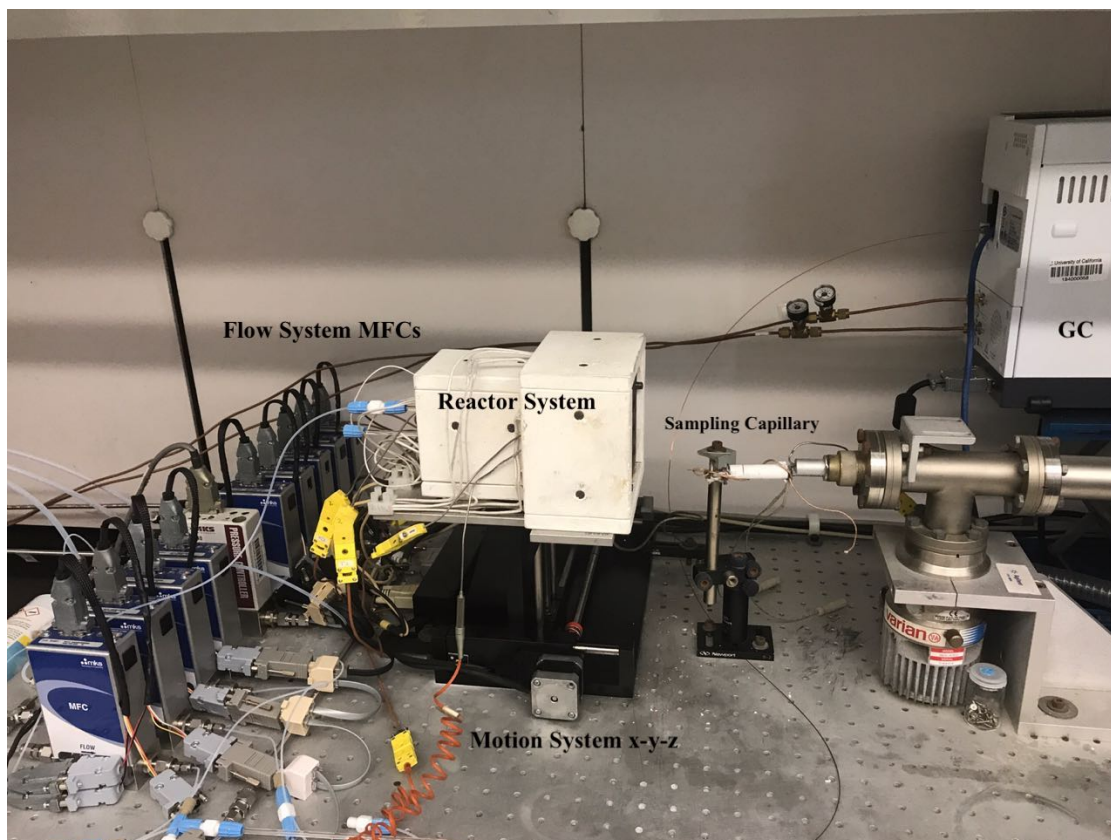


**Figure 5:** High Throughput System

### 2.1.2 Micro-Reactor

The micro-reactor system shown in Figure 6 has multiple components as: A. Each reactor bank with 20 parallel channels (4 banks, total 80 channels); B. Capillary sampling probe; D. Wells containing individual catalyst pellets or powders; E. Temperature controlled heating block; F. Insulation.

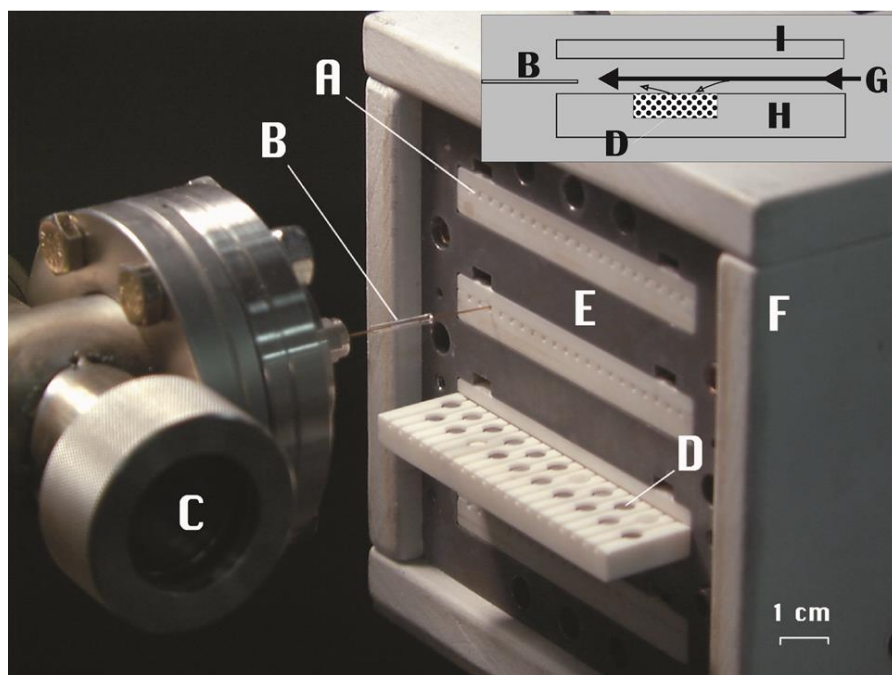


**Figure 6:** High Throughput Micro-Reactor System

The wells containing individual catalysts, in a compacted powder form, are shown in Figure 7. The reactant gas, G, flows over D, the catalyst bed in the well. The capillary probe, B is inserted into the channel for sampling.

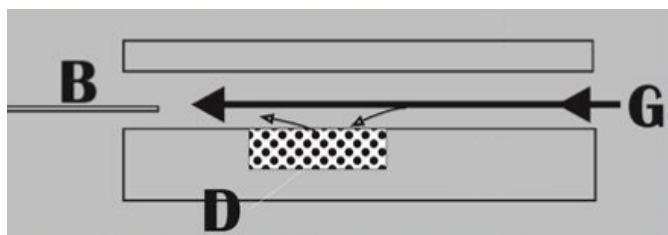


**Figure 7:** Wells Containing Individual Catalyst Pellets or Powders

### 2.1.3 Feed Gas Control System

The mass flow controllers (MFC) from MKS, shown in Figure 8, deliver different pressurized mixture gases and inert gases. There are 10 MFCs, 1-4 control the output of the gas mixture into the reactor system, whereas 5-10 control the gas input from the cylinders. After flow rates are set, all gases are premixed in a mixing tube before they are fed to the reactor. All MFCs are calibrated using a bubble flow meter before being used.

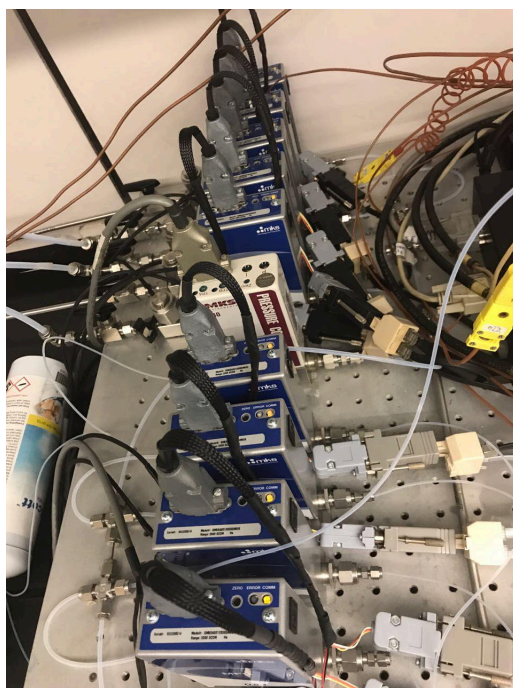


**Figure 8:** Mass Flow Controller Set-up

### 2.1.4 Gas Chromatography System

The effluent from the reactor set-up was analyzed using Agilent micro Gas Chromatography (GC), as shown in Figure 9. There are two columns in micro-GC, column A is a molecular sieve 13X (10 m) that allows the separation of smaller molecules, while column B is a Porapak U column (PPU, 10m) that handles the larger gas molecules. The gas is introduced to the micro-GC system using a  $500\mu\text{m} \times 30\text{cm}$

fused silica capillary connected from the reactor to the pump. For analysis of the gas products, the micro-GC is equipped with a thermal conductivity detector (TCD). The signals produced by the TCD represent retention times and peak areas that are then used in quantitative and qualitative analysis.

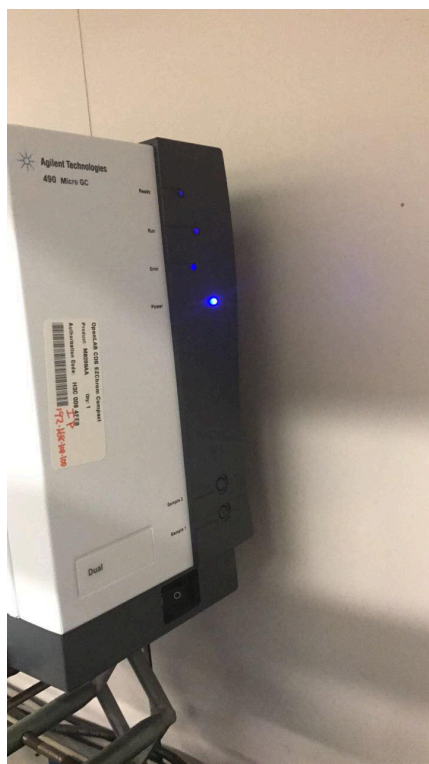


**Figure 9:** Agilent Micro Gas Chromatography (GC)

## 2.2 Experimental Procedure

A specific and consistent procedure was developed for each experiment. The procedure steps are highlighted below:

1. 20 mg of catalyst was crushed, sieved and loaded to the reactor.
2. The loaded catalyst was then reduced under pure H<sub>2</sub> at 400°C (10°C/min) for 2 hours.

3. The temperature of the system was changed to the desired reaction temperature, usually 450°C, under H<sub>2</sub> atmosphere.
4. When the system reaches the desired temperature, the gas feed was switched to the reactant gases, which are 50 vol% H<sub>2</sub> and 50 vol% CO<sub>2</sub> with total flow rate of 12.5 ml/min.
5. Once the catalyst has been on stream for 30 minutes, the first GC injection was withdrawn for analysis.
6. After two and half hours of reaction, the system was cooled down to room temperature and flushed with nitrogen.
7. When the system reaches room temperature, the reacted catalyst was collected.
8. At the end, the reactor was cleaned thoroughly to avoid cross contamination.

### 2.2.1 Catalyst Preparation

All catalysts tested in these experiments were synthesized via incipient wetness impregnation. The pore volume of each support was determined by adding water droplets while stirring, until a water layer starts to form on the surface of the solid. Seven different supports (CeO<sub>2</sub>, MgO, WO<sub>3</sub>, TiO<sub>2</sub>, SiO<sub>2</sub>,  $\alpha$ -Al<sub>2</sub>O<sub>3</sub> and  $\gamma$ -Al<sub>2</sub>O<sub>3</sub>) were impregnated by 6 different metals (Cu, Ni, Fe, Co, Ce and Mn). For example, 10 wt% Cu support on MgO was prepared by dissolving 0.37 g of Cu nitrate salt, Cu(NO<sub>3</sub>)<sub>2</sub> · 2.5H<sub>2</sub>O in water. Then, the solution was added to Magnesium oxide powder, MgO, while stirring. The obtained catalysts were then dried at 110°C (10°C/min) overnight, and calcined at 350°C (10°C/min) for 4 hours. Table 1 shows the list of catalysts prepared for this project.

**Table 1:** Catalyst Prepared for this Project

<b>Catalyst</b>	<b>Catalyst Composition</b>
AZ-1	Cu/CeO <sub>2</sub> (10:90)
AZ-2	Cu/MgO (10:90)
AZ-3	Cu/WO <sub>3</sub> (10:90)
AZ-4	Cu/TiO <sub>2</sub> (10:90)
AZ-5	Cu/SiO <sub>2</sub> (10:90)
AZ-6	Cu/ $\alpha$ -Al <sub>2</sub> O <sub>3</sub> (10:90)
AZ-7	Cu/ $\gamma$ -Al <sub>2</sub> O <sub>3</sub> (10:90)
AZ-8	Cu/MgO (1:99)
AZ-9	Cu/MgO (3:97)
AZ-10	Cu/MgO (5:95)
AZ-11	Cu/MgO (7:93)
AZ-12	Ni/MgO (5:95)
AZ-13	Fe/MgO (5:95)
AZ-14	Co/MgO (5:95)
AZ-15	Ce/MgO (5:95)
AZ-16	Mn/MgO (5:95)

### 2.2.2 Type of Experiments

In order to achieve the objective of this research, different sets of experiments were conducted. These experiments were divided into three sets, which are: study of the

effect of different supports, study of the effect of metal loadings, and study of the effect of different types of metals.

#### *The Effect of Support*

Seven Cu supported catalysts were tested in the high throughput reactor to determine the effect of metal-support interaction and its effect on CO<sub>2</sub> conversion. These catalysts are 10 wt% Cu supported on CeO<sub>2</sub>, MgO, WO<sub>3</sub>, TiO<sub>2</sub>, SiO<sub>2</sub>,  $\alpha$ -Al<sub>2</sub>O<sub>3</sub> and  $\gamma$ -Al<sub>2</sub>O<sub>3</sub>. All these catalysts were tested at the same reaction condition; 450°C, 1 atm and 12.5 ml/min.

#### *The Effect of Metal Loading*

10 wt% Cu on MgO catalyst was determined to be the best catalyst in term of CO<sub>2</sub> conversion. Different Cu loading catalysts were tested to determine the optimum metal loading in terms of CO<sub>2</sub> conversion. The catalysts prepared for this set of experiments are 1 wt% Cu, 3 wt% Cu, 5 wt% Cu, 7 wt% Cu and 10 wt% Cu.

#### *The Effect of Different Type of Metals*

After the best support and optimum metal loading were determined, different metals were tested to study their effect on CO<sub>2</sub> conversion. Seven different metals were supported on MgO with 5 wt% of each metal. These metals are Cu, Ni, Fe, Co, Ce and Mn.



### CHAPTER 3. EXPERIMENTAL RESULTS AND DISCUSSION

The results of this project were compared to the equilibrium data obtained from Aspen Plus simulations. A Gibbs reactor was used in the simulation with an NRTL based thermodynamic description; the reaction conditions used were similar to the experimental ones, 450°C, 1 atm, 1:1 H<sub>2</sub>:CO<sub>2</sub> ratio, and a feed of 1 mole of CO<sub>2</sub> and 1 mole of H<sub>2</sub>. The schematic of the Gibbs reactor is shown in Figure 10.

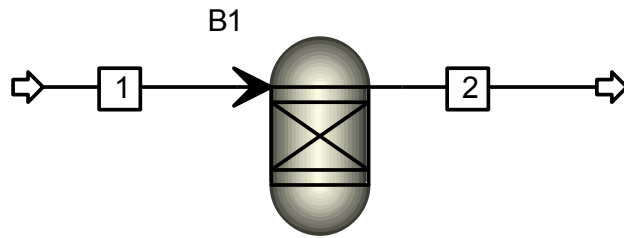


**Figure 10:** Schematic of the Gibbs Reactor

CO<sub>2</sub> conversion at equilibrium is shown in Figure 11. The CO<sub>2</sub> conversion at equilibrium is almost constant at 25% as the temperature increases until it reaches 450°C. However, when the temperature increases above 450°C, the CO<sub>2</sub> conversion increases significantly to reach the maximum conversion of 50% at 800°C. The CO selectivity at equilibrium is less than 5% at temperatures less than 400°C. As the temperature increases from 450°C to 800°C, the selectivity increases from 16% to 99%.

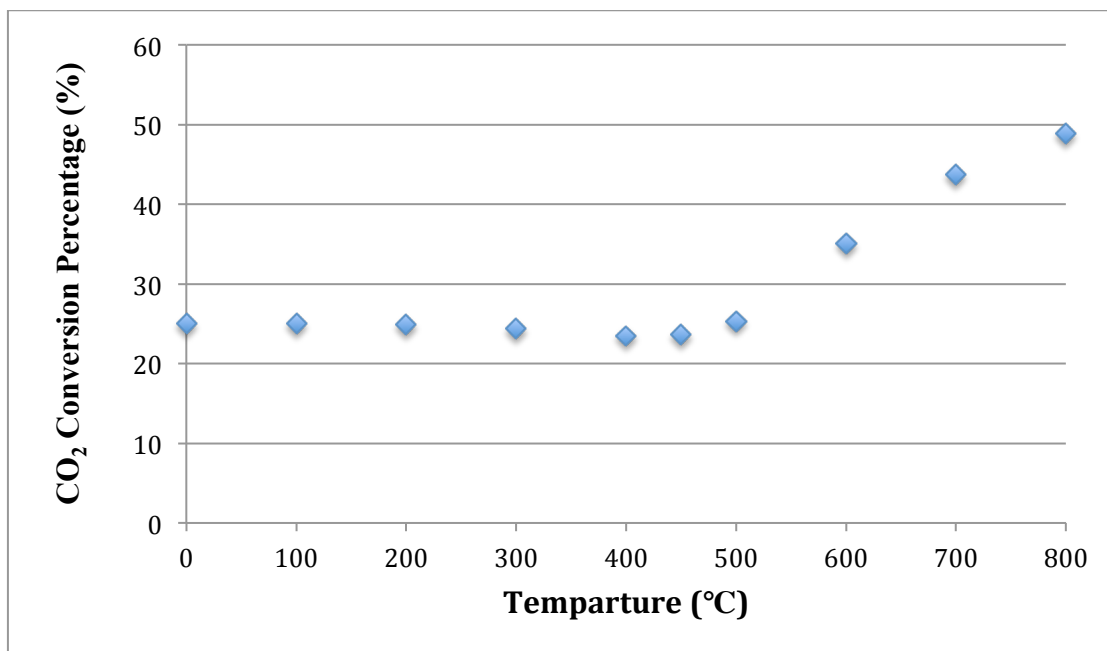


**Figure 11:** CO<sub>2</sub> Equilibrium Conversion

All of the experimental results in this project are reported in terms of CO<sub>2</sub> conversion and CO selectivity, these two terms were calculated using the following equations:

$$\text{CO}_2 \text{ Conversion \%} = \frac{\text{CO}_2(\text{feed}) - \text{CO}_2(\text{out})}{\text{CO}_2(\text{feed})} \times 100\%$$

$$\text{CO selectivity \%} = \frac{\text{CO}(\text{out})}{\text{CO}_2(\text{feed}) - \text{CO}_2(\text{out})} \times 100\%$$

All the catalysts tested for this project were characterized by BET analysis (Micromeritics ASAP 2020 using N<sub>2</sub>) to determine the surface area of the catalyst. The samples were degassed under N<sub>2</sub> atmosphere at 180°C overnight. X-ray Diffraction (XRD) was used to understand the morphology and crystallinity of the catalyst. The XRD measurements were made using a Rigaku MiniFlex II diffractometer, which used a Cu K $\alpha$  X-ray (40 ma, 44 kV) operating with focused beam geometry and a divergence slit of 2/3 degree, a scan speed of 5 deg/min and the samples were scanned from 20-80° in 2 $\theta$  range.

Energy Dispersive x-ray Spectroscopy (EDS) was used to check the percentage of metal loaded into the support. Table 2 shows the actual metal percentage loaded for each prepared catalyst.

**Table 2:** The Actual Metal Percentage Loaded for each Prepared Catalyst

<b>Catalyst</b>	<b>Catalyst Composition</b>	<b>Actual Composition by EDS</b>
AZ-1	Cu/CeO <sub>2</sub> (10:90)	9.8:90.2
AZ-2	Cu/MgO (10:90)	9.9:90.1
AZ-3	Cu/WO <sub>3</sub> (10:90)	10.1:89.9
AZ-4	Cu/TiO <sub>2</sub> (10:90)	9.8:90.2
AZ-5	Cu/SiO <sub>2</sub> (10:90)	10.0:90.0
AZ-6	Cu/ $\alpha$ -Al <sub>2</sub> O <sub>3</sub> (10:90)	9.9:90.1
AZ-7	Cu/ $\gamma$ -Al <sub>2</sub> O <sub>3</sub> (10:90)	10.0:90.0
AZ-8	Cu/MgO (1:99)	0.99:99.1
AZ-9	Cu/MgO (3:97)	3:97.0
AZ-10	Cu/MgO (5:95)	5.0:95.0
AZ-11	Cu/MgO (7:93)	6.9:93.1
AZ-12	Ni/MgO (5:95)	5.0:95.0
AZ-13	Fe/MgO (5:95)	5.0:95.0
AZ-14	Co/MgO (5:95)	5.1:94.9
AZ-15	Ce/MgO (5:95)	4.9:95.1
AZ-16	Mn/MgO (5:95)	5.0:95.0

### 3.1 The Effect of Support

The first part of this project was to select the most active support for Cu metal catalyst in term of CO<sub>2</sub> conversion. The results of CO<sub>2</sub> conversion for different supported Cu catalysts and the equilibrium conversion are shown in Figure 12. Cu supported on WO<sub>3</sub> (AZ-3), TiO<sub>2</sub> (AZ-4) and SiO<sub>2</sub> (AZ-5) showed almost zero CO<sub>2</sub> conversion at 450°C, whereas the best catalyst was support on MgO (AZ-2) with a conversion of around 10%, which is about 40% of equilibrium CO<sub>2</sub> conversion. The catalysts supported on  $\alpha$ -Al<sub>2</sub>O<sub>3</sub> (AZ-6) and  $\gamma$ -Al<sub>2</sub>O<sub>3</sub> (AZ-7) showed a CO<sub>2</sub> conversion less than 1% and around 4%, respectively.

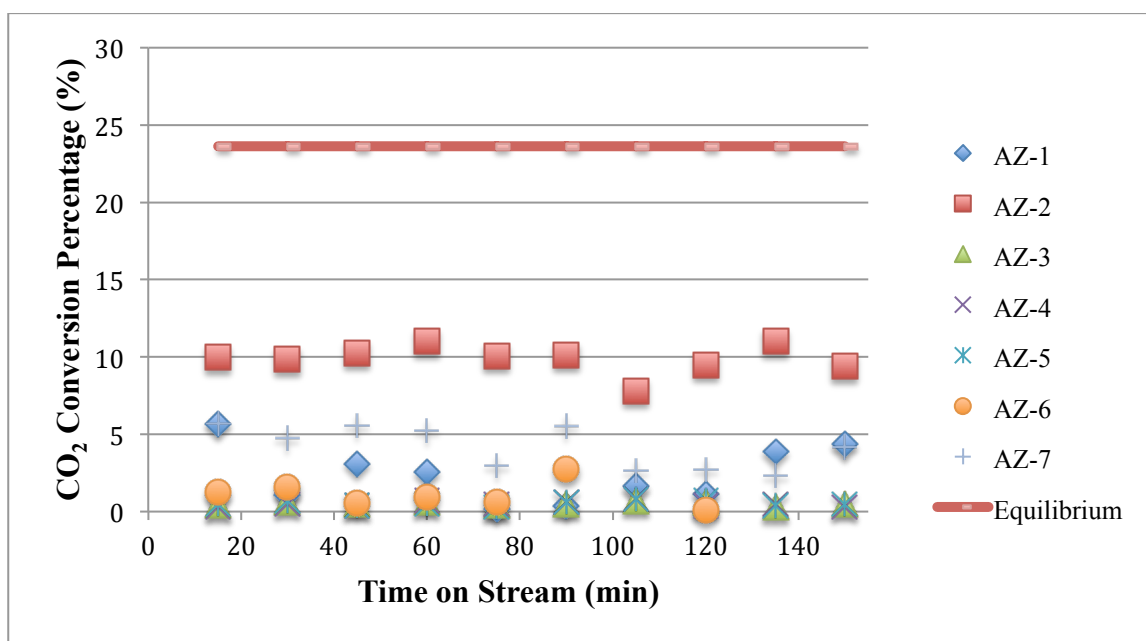


**Figure 12:** CO<sub>2</sub> Conversion for Different Support

The CO selectivity of different supported catalysts is shown in Figure 13. The catalysts supported on CeO<sub>2</sub> (AZ-1) and MgO (AZ-2) showed a similar CO selectivity around 30%. The catalysts supported on WO<sub>3</sub> (AZ-3), TiO<sub>2</sub> (AZ-4) and SiO<sub>2</sub> (AZ-5) displayed little traces of CO products in the outlet stream, whereas the catalysts supported

on  $\alpha$ -Al<sub>2</sub>O<sub>3</sub> (AZ-6) and  $\gamma$ -Al<sub>2</sub>O<sub>3</sub> (AZ-7) showed a similar CO selectivity at 60%, which is the highest obtained CO selectivity for different supports.

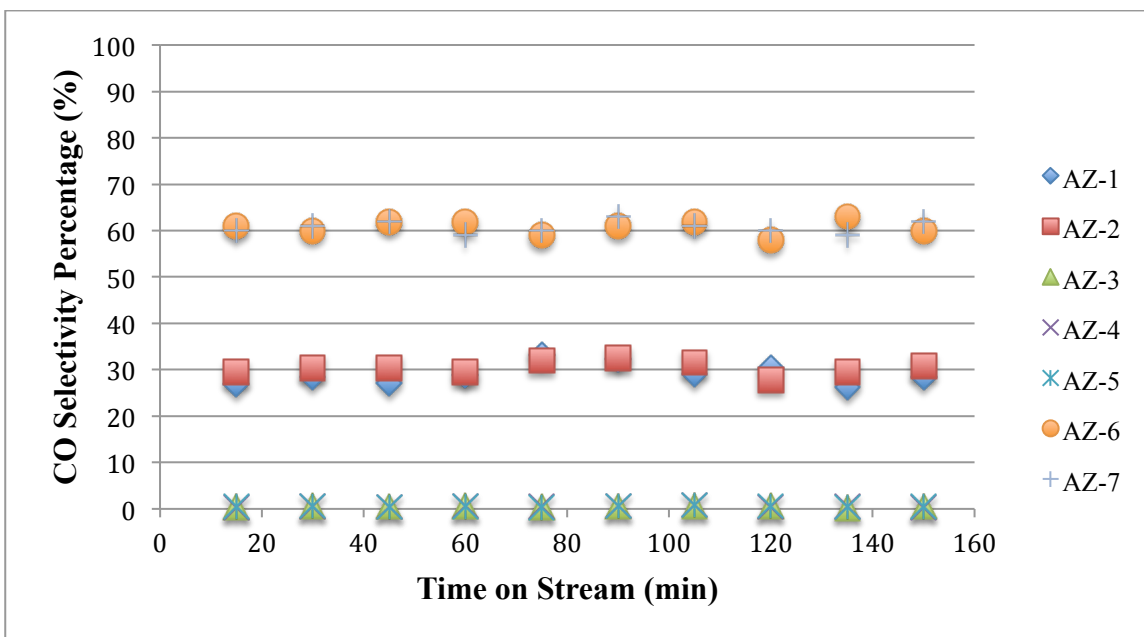


**Figure 13:** CO Selectivity for Different Support

In order to understand the catalyst structure and surface chemistry, BET and XRD analysis were performed. It is known that usually a high surface area indicates a high catalytic activity and BET analysis showed that Cu/SiO<sub>2</sub> (AZ-5) has the highest surface area of 250.3 m<sup>2</sup>/g; however, this does not reflect on its activity as it showed little CO<sub>2</sub> conversion. Figure 14 shows the XRD pattern for Cu/SiO<sub>2</sub> (AZ-5) and it indicates that the sample was amorphous, which could be the reason for its low activity.

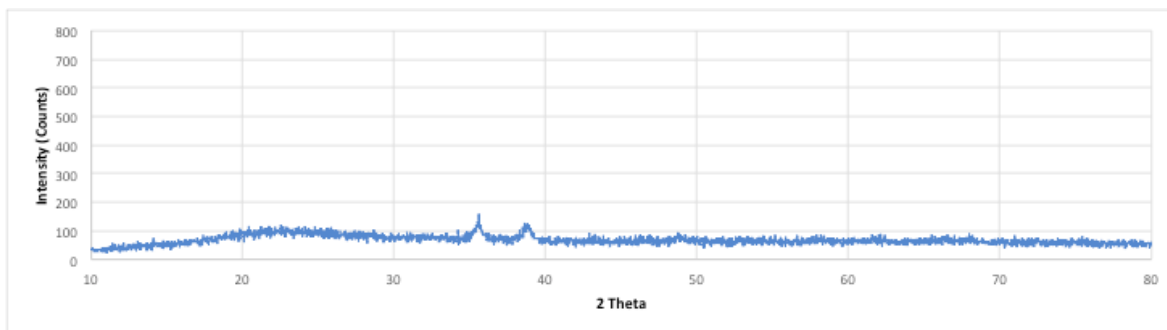


**Figure 14:** XRD Spectrum for 10 wt% Cu/SiO<sub>2</sub>

The Cu/MgO (AZ-2) that showed the highest CO<sub>2</sub> conversion and moderate CO selectivity has a surface area of 29.7 m<sup>2</sup>/g. Figure 15 shows the XRD pattern for Cu/MgO (AZ-2), which indicates that the sample is crystalline with an intense peak for an MgO particle size of 202.1 nm.

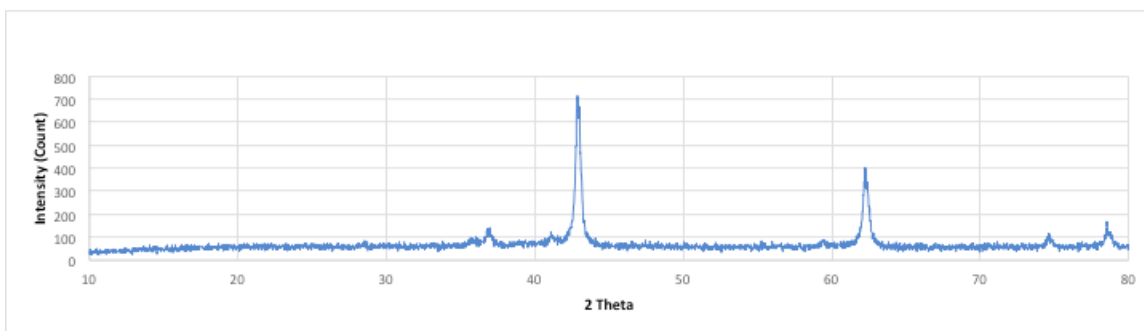


**Figure 15:** XRD Spectrum for 10 wt% Cu/MgO

### 3.2 The Effect of Metal Loading

Based on the results, the best support for Cu based catalysts for RWGS reaction was determined to be MgO. The optimum metal loading for Cu catalyst was investigated by varying the Cu weight percent from 1% to 10%, and Figure 16 shows the resulted CO<sub>2</sub> conversion. The optimum amount of Cu loading was found to be 5 wt% (AZ-10), which resulted in CO<sub>2</sub> conversion of around 20%, which is 83% of equilibrium CO<sub>2</sub> conversion. The second best catalyst was 3 wt% (AZ-9) Cu loading, which resulted in 17% CO<sub>2</sub>

conversion. When 10 wt% (AZ-2) Cu loading was used, it showed the lowest conversion at 10% compared to other tested catalysts.

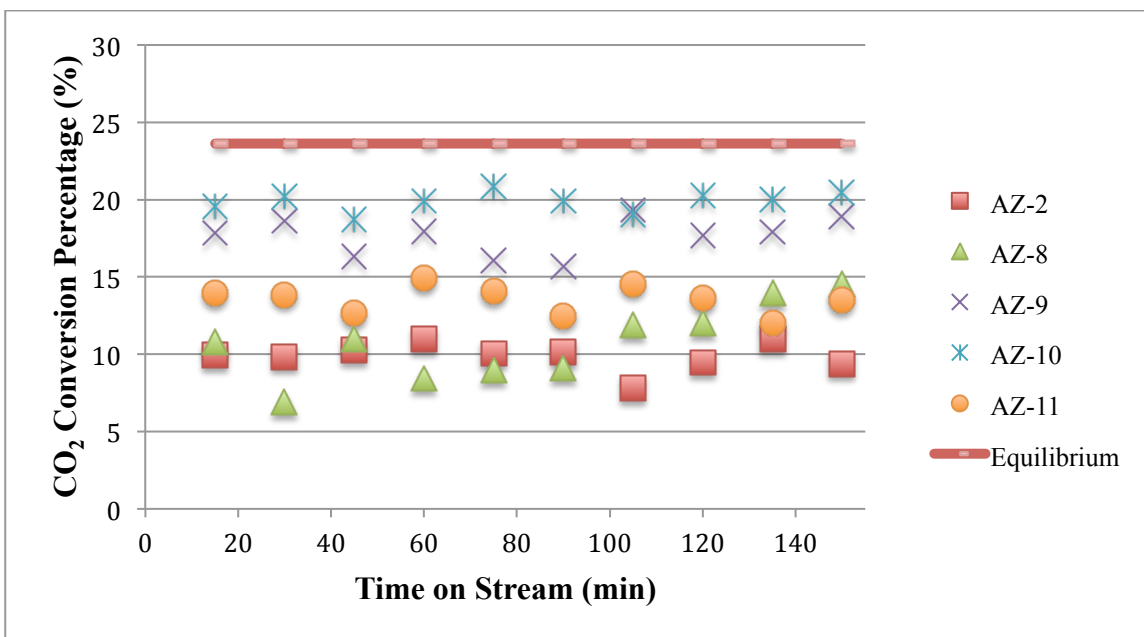


**Figure 16:** CO<sub>2</sub> Conversion for Different Metal Loading

As shown in Figure 17, 5 wt% (AZ-10) Cu catalyst showed the highest CO selectivity at 75%, followed by 3 wt% (AZ-9) Cu catalyst at 61% CO selectivity. The lowest CO selectivity, 23% CO selectivity, was achieved with 7 wt% (AZ-11) Cu catalyst. Also, Figure 17 shows that 10 wt% (AZ-2) Cu catalyst has a selectivity of 30%, where 1 wt% (AZ-8) Cu catalyst shows a CO selectivity of 26%.

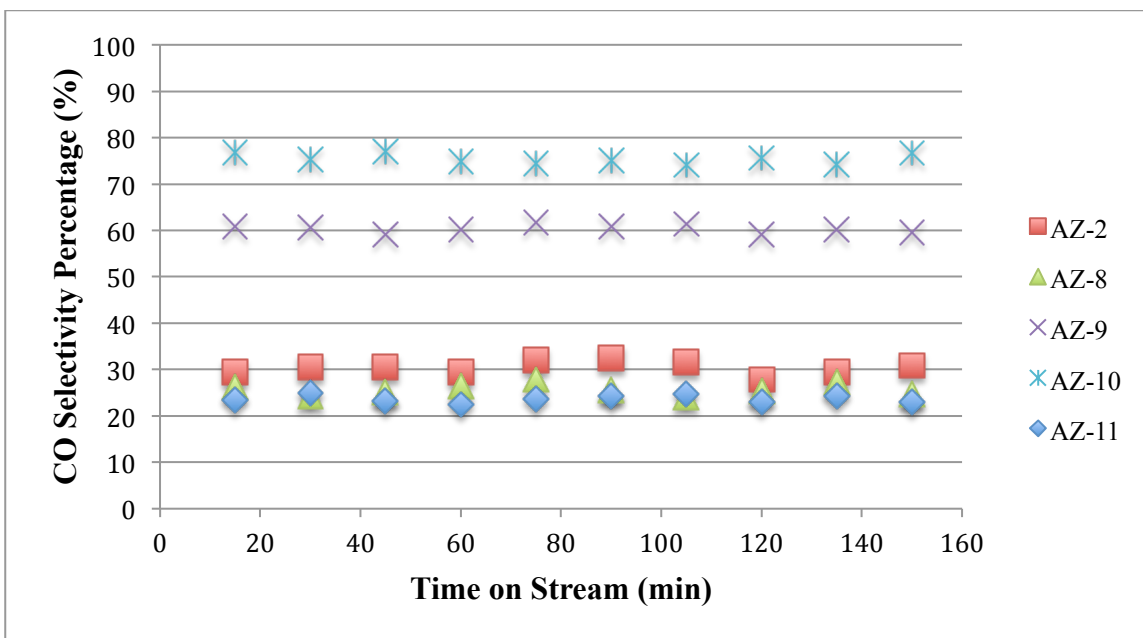


**Figure 17:** CO Selectivity for Different Metal Loading

### 3.3 The Effect of Different Types of Metals

Once the best supports and optimum metal loadings were investigated and determined, different single metals were tested for the best CO<sub>2</sub> conversion and CO selectivity, as shown in Figure 18. All the tested catalysts were 5 wt% supported on MgO and Cu/MgO (AZ-10) was found to be the best catalyst for the RWGS reaction with 20% CO<sub>2</sub> conversion, followed by Co/MgO (AZ-14) with a CO<sub>2</sub> conversion of 9%. Figure 18 indicated that Ni (AZ-12) and Mn (AZ-17) have similar CO<sub>2</sub> conversion at 4.5%, while Fe (AZ-13) showed only 2.5% CO<sub>2</sub> conversion. Ce/MgO (AZ-15) did not show any CO<sub>2</sub> conversion with the exception of some traces of CO<sub>2</sub>.



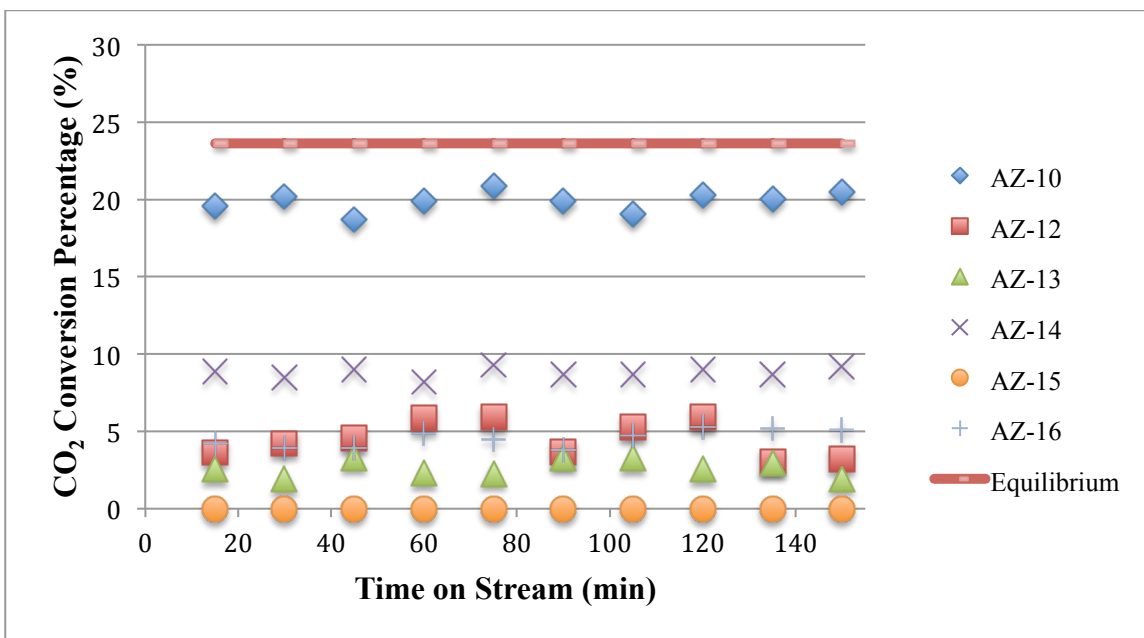


**Figure 18:** CO<sub>2</sub> Conversion for Different Metals

The CO selectivity of different metals tested is shown in Figure 19 below. Ni/MgO (AZ-12) showed the highest CO selectivity amongst all of the tested catalysts, with a selectivity of 90%, followed by Fe/MgO (AZ-13) and Co/MgO (AZ-14) with a similar CO selectivity of around 87.5%. Also, Figure 19 shows that Cu/MgO (AZ-10) and Mn/MgO (AZ-17) had a CO selectivity of 75% and 39%, respectively.

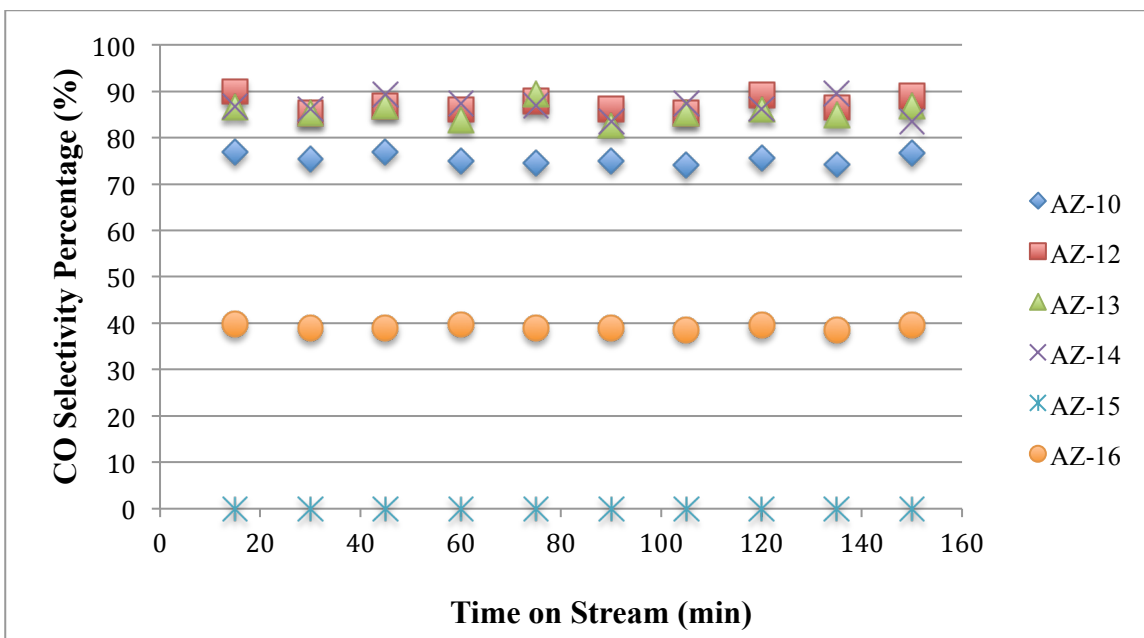


**Figure 19:** CO Selectivity for Different Metals

BET analysis shows that the 5wt % Cu/MgO (AZ-10), which showed the highest CO<sub>2</sub> conversion, has surface area of 44.6 m<sup>2</sup>/g which is higher than the second-best catalyst Co/MgO (AZ-14) with particle size of 134.5 nm. Also, Figure 20 shows the XRD spectrum which indicates that the MgO peaks are more pronounced than 10 wt% Cu/MgO (AZ-2) which could explain why Cu/MgO (AZ-10) is the most active catalyst among the tested catalysts.

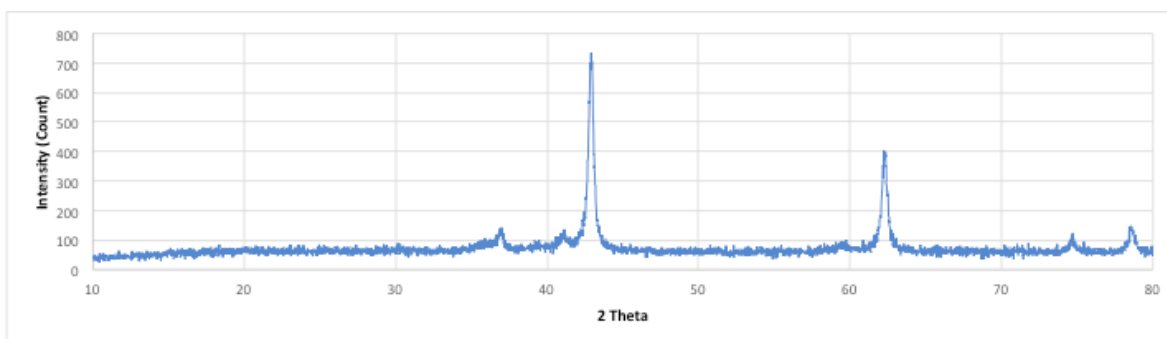


**Figure 20:** XRD Spectrum for 5 wt% Cu/MgO

## CHAPTER 4. CONCLUSIONS AND RECOMMENDATIONS

### 4.1 Conclusions

After the analysis and discussion of all experimental results obtained from this research, several conclusions can be made regarding the best support for RWGS reaction, optimum metal loading and effect of different metals on CO<sub>2</sub> conversion and CO selectivity. Sixteen different supported metal catalysts were synthesized successfully via incipient wetness impregnation. All the experiments were conducted under the same reaction conditions, 450°C, 1 atm, 1:1 H<sub>2</sub>:CO<sub>2</sub> and 12.5 ml/min.

In the first stage of this research, seven different supports were tested for Cu based catalyst and it was found that MgO support possessed the highest CO<sub>2</sub> conversion of 10% and 30% CO selectivity. The reason for its high activity is believed to be due to the crystallinity of the material.

The second stage was to optimize the metal loading specifically for Cu, which was done by testing five different metal loadings, 1 wt%, 3 wt%, 5 wt%, 7 wt% and 10 wt%. It was found that 5 wt% Cu support on MgO achieved the highest CO<sub>2</sub> conversion of 20% with a CO selectivity of 75%.

The last stage of this research was to test six different supported metals, Cu, Ni, Fe, Co, Ce and Mn, to investigate their effect on CO<sub>2</sub> conversion and CO selectivity. Cu support catalyst was the best catalyst among the tested ones, with a CO<sub>2</sub> conversion of 20% and CO selectivity of 75%; followed by Co based catalyst supported on MgO.

Based on the results of this research, it can be concluded that Cu based, MgO supported catalyst is the best catalyst system for the RWGS reaction at the tested conditions.

## 4.2 Recommendations for Future Work

The results of the current research using Cu supported catalysts look promising to reduce CO<sub>2</sub> emissions into the atmosphere via the RWGS reaction. However, more studies should be conducted in the future to further optimize the catalyst before it can be used commercially. A list of recommended future studies are outlined below:

- More characterizations such as TEM, SEM and TPR to understand the physical and chemical structure of the tested catalysts to better identify the active sites of the catalyst.
- Test Cu based catalysts under different reaction conditions, such as different reaction temperatures, space velocities, feed compositions, and pressures.
- Test the effect of different preparation methods and different catalyst systems, such as binary and ternary systems.

## REFERENCES

- [1] Scripps Institution of Oceanography. (2018). Mauna Loa Record. [online] Available at: [http://scrippsco2.ucsd.edu/graphics\\_gallery/mauna\\_loa\\_record/mauna\\_loa\\_record](http://scrippsco2.ucsd.edu/graphics_gallery/mauna_loa_record/mauna_loa_record).
- [2] Intergovernmental Panel on Climate Change (IPCC) Climate Change 2014 Synthesis Report Summary for Policymakers
- [3] International Energy Agency (IEA). (2017). Key World Energy Statistics 2017. [online] Available at: <https://webstore.iea.org/key-world-energy-statistics-2017>.
- [4] Intergovernmental Panel on Climate Change (IPCC) Climate Change 2014 Mitigation of Climate Change
- [5] Carbon Cycling and Biosequestration Integrating Biology and Climate Through Systems Science. (2018). U.S. Department of Energy.
- [6] Carbon Capture & Storage Association (CCSA). (2018) What is CCS?. [online] Available at: <http://www.ccsassociation.org/what-is-ccs/>.
- [7] E. A. Quadrelli, G. Centi, J.-L. Duplan, and S. Perathoner, “Carbon dioxide recycling: emerging large-scale technologies with industrial potential.” *ChemSusChem*, vol. 4, pp. 1194–215, Sep. 2011.
- [8] C.-H. Huang, “A Review: CO<sub>2</sub> Utilization,” *Aerosol Air Qual. Res.*, pp. 480–499, 2014.
- [9] W. Wang, S. Wang, X. Ma and J. Gong, “Recent advances in catalytic hydrogenation of carbon dioxide”, *Chem. Soc. Rev.*, 2011, 40, 3703.

- [10] P. Panagiotopoulou, D. I. Kondarides and X. E. Verykios, “Mechanistic aspects of the selective methanation of CO over Ru/TiO<sub>2</sub> catalyst”, *Catal. Today*, 2012, 181, 138–147.
- [11] P. Kaiser, R. B. Unde, C. Kern and A. Jess, “Production of Liquid Hydrocarbons with CO<sub>2</sub> as Carbon Source based on Reverse Water-Gas Shift and Fischer-Tropsch Synthesis”, *Chem.-Ing.-Tech.*, 2013, 85, 489.
- [12] G. Centi and S. Perathoner, “Opportunities and prospects in the chemical recycling of carbon dioxide to fuels”, *Catal. Today*, 2009, 148, 191.
- [13] F. E. Kruis, H. Fissan, and A. Peled, “Synthesis of nanoparticles in the gas phase for electronic, optical and magnetic applications—a review,” *J. Aerosol Sci.*, vol. 29, no. 5–6, pp. 511–535, Jun. 1998.
- [14] G. Centi and S. Perathoner, “Opportunities and prospects in the chemical recycling of carbon dioxide to fuels,” *Catal. Today*, vol. 148, no. 3–4, pp. 191–205, Nov. 2009.
- [15] S. S. Kim, K. H. Park, and S. C. Hong, “A study of the selectivity of the reverse water– gas-shift reaction over Pt/TiO<sub>2</sub> catalysts,” *Fuel Process. Technol.*, vol. 108, pp. 47–54, Apr. 2013.
- [16] S. S. Kim, H. H. Lee, and S. C. Hong, “A study on the effect of support’s reducibility on the reverse water-gas shift reaction over Pt catalysts,” *Appl. Catal. A Gen.*, vol. 423–424, pp. 100–107, May 2012.
- [17] K. Oshima, T. Shinagawa, Y. Nogami, R. Manabe, S. Ogo and Y. Sekine, “Low temperature catalytic reverse water gas shift reaction assisted by an electric field”, *Catal. Today*, 2014, 232, 27.

- [18] L. Wang, S. Zhang, and Y. Liu, "Reverse water gas shift reaction over Co-precipitated Ni- CeO<sub>2</sub> catalysts," *J. Rare Earths*, vol. 26, pp. 66–70, 2008.
- [19] B. Lu and K. Kawamoto, *Mater. Res. Bull.*, 2014, 53, 70.
- [20] Y. Liu and D. Liu, *Int. J. Hydrogen Energy*, 1999, 24, 351.
- [21] N. Takezawa, T. Hiroyuki, M. Shimokawabe, and H. Kobayashi, "Methanation of Carbon Dioxide: Preparation of Ni/MgO Catalysts and Their Performance," *Appl. Catal. A Gen.*, vol. 23, pp. 291–298, 1986.
- [22] J. C. Matsubu, V. N. Yang and P. Christopher, "Isolated metal active site concentration and stability control catalytic CO<sub>2</sub> reduction selectivity", *J. Am. Chem. Soc.*, 2015, 137, 3076.
- [23] T. Inoue, T. Iizuka and K. Tanabe, "Hydrogenation of carbon dioxide and carbon monoxide over supported rhodium catalysts under 10 bar pressure", *Appl. Catal.*, 1989, 46, 1.
- [24] M. R. Gogate and R. J. Davis, "Comparative study of CO and CO<sub>2</sub> hydrogenation over supported Rh–Fe catalysts" , *Catal. Commun.*, 2010, 11, 901.
- [25] K. K. Bando, K. Soga, K. Kunimori and H. Arakawa, "Effect of Li additive on CO<sub>2</sub> hydrogenation reactivity of zeolite supported Rh catalysts", *Appl. Catal., A*, 1998, 175, 67–81.
- [26] Y. Liu and D. Liu, "Study of bimetallic Cu-Ni/ gamma Al<sub>2</sub>O<sub>3</sub> catalysts for carbon dioxide hydrogenation," *J. Hydrog. Energy*, vol. 24, pp. 351–354, 1999.
- [27] D.-W. Jeong, W.-J. Jang, J.-O. Shim, W.-B. Han, H.-S. Roh, U. H. Jung, and W. L. Yoon, "Low-temperature water–gas shift reaction over supported Cu catalysts," *Renew. Energy*, vol. 65, pp. 102–107, May 2014.

- [28] C. S. Chen, J. H. Lin, J. H. You and C. R. Chen, “Properties of Cu(thd)<sub>2</sub> as a Precursor to Prepare Cu/SiO<sub>2</sub> Catalyst Using the Atomic Layer Epitaxy Technique”, *J. Am. Chem. Soc.*, 2006, 128, 15950–15951.
- [29] C.-S. Chen, W.-H. Cheng and S.-S. Lin, “Study of reverse water gas shift reaction by TPD, TPR and CO<sub>2</sub> hydrogenation over potassium-promoted Cu/SiO<sub>2</sub> catalyst” ,*Appl. Catal., A*, 2003, 238, 55.
- [30] M. A. Edwards, D. M. Whittle, C. Rhodes, A. M. Ward, D. Rohan, M. D. Shannon, G. J. Hutchings, and C. J. Kiely, “Microstructural studies of the copper promoted iron oxide/chromia water-gas shift catalyst,” *Phys. Chem. Chem. Phys.*, vol. 4, no. 15, pp. 3902–3908, Jul. 2002.
- [31] F. S. Stone and D. Waller, “Cu-ZnO and Cu-ZnO/Al<sub>2</sub>O<sub>3</sub> catalysts for the reverse water-gas shift reaction. The effect of the Cu/Zn ratio on precursor characteristics and on the activity of the derived catalysts”, *Top. Catal.*, 2003, 22, 305–318.
- [32] C. S. Chen, J. H. Lin, J. H. You and C. R. Chen, “Properties of Cu(thd)<sub>2</sub> as a Precursor to Prepare Cu/SiO<sub>2</sub> Catalyst Using the Atomic Layer Epitaxy Technique” , *J. Am. Chem. Soc.*, 2006, 128, 15950–15951.